MMX Locomotion Subsystem: mechanics for extraterrestrial low gravity drive

Viktor Langofer[1]
Viktor.Langofer@dlr.de

Ralph Bayer[1]
Ralph.Bayer@dlr.de

Alexander Kolb[1]
Alexander.Kolb@dlr.de

Kaname Sasaki[2]
Kaname.Sasaki@dlr.de

[1] German Aerospace Center (DLR)
Institute of Robotics and Mechatronics
Münchener Str. 20
82234 Weßling

[2] German Aerospace Center (DLR)
Institute of Space Systems
Robert-Hooke-Str. 7
28359 Bremen

Abstract— The advent of exploring low-gravity environments gives the opportunity to land rovers on celestial bodies without any landing platform and perform manipulative tasks under mostly unknown conditions. In addition to common loads, for example vibration, operation and thermal loads, the rover will face also impact loads during touchdown. This circumstance requires additional mechanisms to protect exposed parts, like the legs and wheels of a rover. Previous research attaches the wheels to the rover body or the landing platform through cup-cone interfaces at the wheel hub, which leads to unfavorable force distribution at the wheel rim in certain load cases, especially if the wheel represents the first point of contact during touchdown. This paper gives a detailed description in the mechanical design and testing of the locomotion subsystem (LSS) of the Martian Moons eXploration (MMX) rover. As the rover will fall to the moon Phobos unprotected and without any landing platform, the exposed locomotion subsystem has a high probability of being the initial contact point at touchdown. Besides the drivetrains and thermal hardware, a novel hold down and release mechanism (HDRM) will be introduced as an integral part of the locomotion subsystem. The HDRM is realized using three support structures at the wheel rim and one fixation in the wheel axis. In this way, the exposed locomotion subsystem will be stabilized in described load cases, since each support structure forms a closed kinematic loop with the wheel and the central fixation in stowed configuration. This approach leads to vibration and impact resistant behavior.

Table of Contents

1. Introduction

The sample return mission, Martian Moons eXploration (MMX), of the Japan Aerospace Agency (JAXA) carries a rover on its way, which will be deployed as a scout on Phobos to perform several scientific tasks during the mission. The deployment aims to ballistically descend the MMX rover on the surface of Phobos and start with its scientific objectives after uprighting with the MMX Rover's Locomotion Subsystem (LSS). The latter is a contribution by the Robotics and Mechatronics Center (RMC) of the German Aerospace Center (DLR) and objective of this paper. The subsystem is an integral part of the MMX rover and provides the link to interact physically with the surface of Phobos in milli-g environment. Not only is it a technical demonstration for driving at low gravity, in addition it serves as a sunpointing device for the solar arrays and supports multiple scientific objectives: e.g. the positioning of the internal scientific payload relative to the surface of Phobos or the direct interaction of the surface regolith to give informations on its characteristics.

The design of LSS is an iterative process, started from 2019 with a concept phase to evaluate different drivetrain strategies and completed in 2022 with the flight model. Thus, the contribution of this paper is to present iteration steps of the system as a result of intensively testing and simulation, as well as the final mechanical design of the LSS in detail as it is supposed to fly to the martian moon Phobos.

2. System Design

In previous publications [1], [2] and [3], the essential specifications derived from the mission needs are presented. Furthermore, general insights to the design and development of the different models of the LSS are given. The following presents an in-depth view on the mechanical design of the flight model. An overview is given by Figure 1, which constitute the LSS in four separable sub-components: a motor unit, a shoulder, a leg and an HDRM. The units are designed to be self-contained, which offers the opportunity to verify a proper function, before being integrated. In the following, the sub-components are described and specific design decisions will be discussed.

Motor unit

The motor unit of the LSS is a reused component with many years of continuously adaptions and improvements within the terrestrial and extraterrestrial (see [4], [5] and [6]) development of the Institute of Robotics and Mechatronics (DLR). The presented motor unit, shown in Figure 2, is designed for use in space applications with demand on operation at very slow movements under low temperatures. The motor unit comprises a stator/rotor element, several bearings, a sealing, two gear stages, a heater and a backshell for commutation. The bearings were choosen in a dissimilar material and dry lubricant approach, where the rings (raceways coated with silver) are made of 1.4108, the balls are from Si_3N_4 and the snap cage is made of Vespel SP3. In this way possible cold welding issues are avoided. Compared to lubricated bearings a higher friction is taken into account at moderate temperature
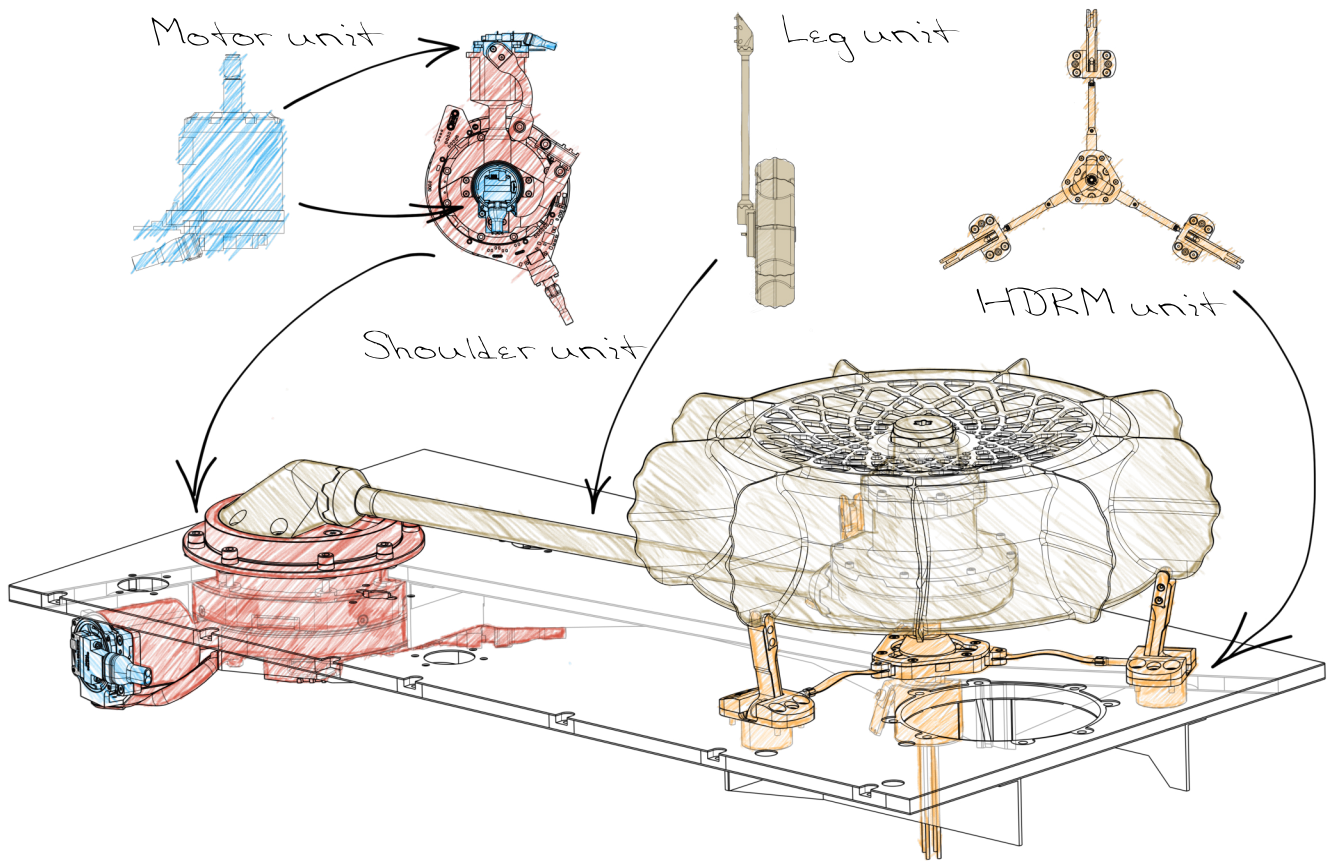
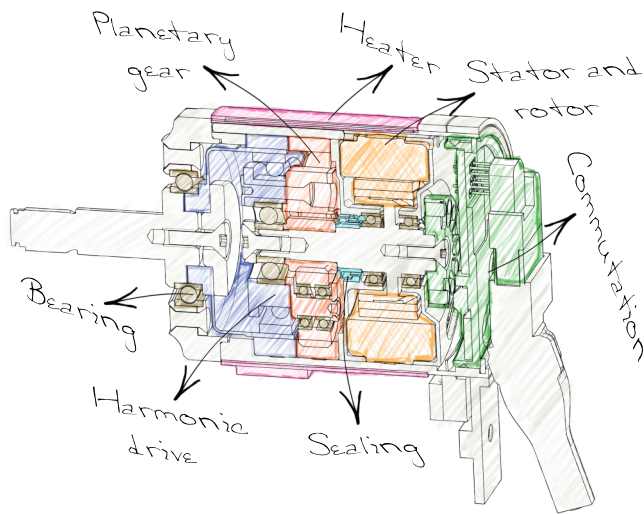**Figure 1**: Overview of the components and assembled state of a locomotion unit on a chassis side panel.

Figure 2: Motor unit

additive for tribological and cryogenic space applications. The material combination provides a dry run capability for extreme cold conditions and the absence of cold welding issues. The output, in this case the carrier of the three planets, is directly attached to the wavegenerator of the harmonic drive through a safe rivet connection, driving the next stage in a compact form factor. The harmonic drive is a space graded version with a 1:100 reduction and is lubricated with Fomblin Z25 and Braycote 602EF. The required lubrication limits the minimal operational temperature to −80 °C and leads to an increase in friction as the temperature gets lower and is subject to several studies (e.g. [4] and [7]). However, the absolute minimal operational temperature requirement of the motor units are −40 °C, which is mainly limited by the rated temperature range of the commutation hall sensors. Together with the need of a high transmission ratio for very slow movements, the avoidance of stiction caused by solidifying grease is achieved through a correspondingly small diameter of the sun in the planetary gearing compared to the effective radius of friction forces in the harmonic drive [1]. In summary the motor unit provides on the output a total reduction ratio of 1:500, has a diameter of 27 mm and weighs approximately 80 g. The non-operational storage temperature is tested successfully down to −150 °C. In addition, the nominal torque is mainly related to the harmonic drive and is rated with 0.9 Nm and peak torques of 1.8 Nm at the gear output of the motor unit. In relation to the mission needs and qualification requirements, the motor is tested during several intermediate tests, especially within the performance test (see Section 3) of the qualification campaign. In general torques until 1.1 Nm, speeds up to 6 °/s and motor temperatures from

ranges, but a constant one at a broad temperature range, especially at cryogenic temperatures. The sealing is designed in a labyrinth approach to not introduce any additional resistive torque at the input of the first planetary gear stage (ratio 1:5). The sun and ring gear of the planetary gearbox is made of 1.4548 stainless steel in condition H1150 for superior performance in cold environment. The planets are made of TECASINT 2391, a highly optimized polyimide with MoS2
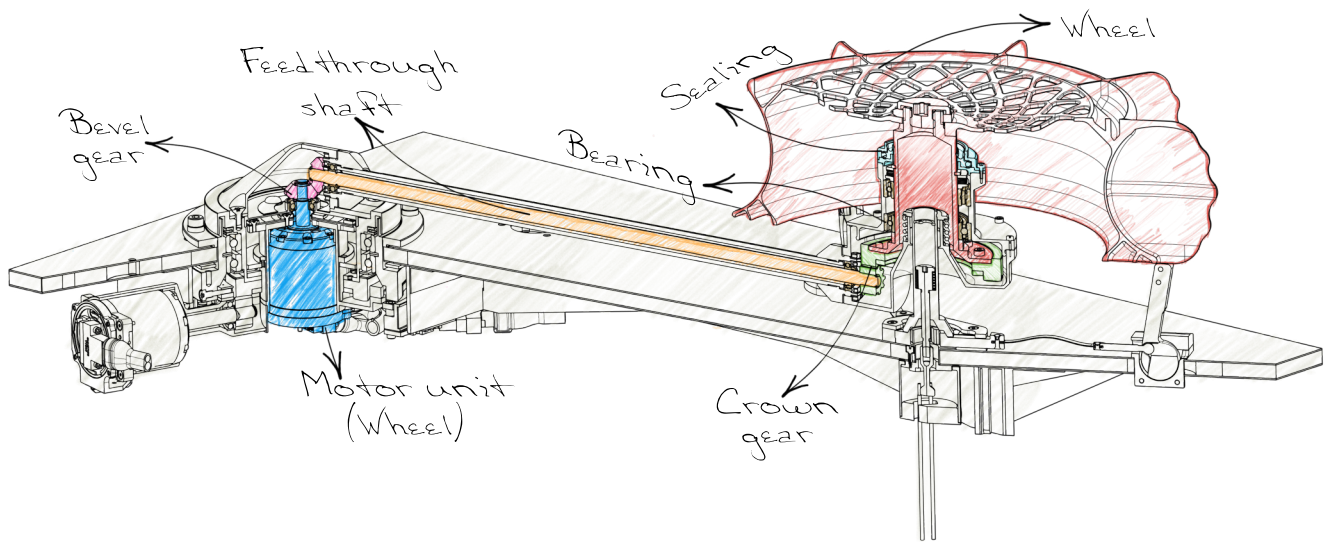
2

Figure 3: Wheel drivetrain of Locomotion Subsystem

80 °C to −35 °C were set within the specified tests. Further out-of-specs tests confirmed the capability to run reliably in six-step commutation down to −40 °C and in a stepper mode down to −60 °C.

Drivetrain

The LSS consists of two drivetrains: one driving the shoulder joint and one driving the wheel. The shoulder drivetrain is used for the uprighting after touchdown, the alignment of the rover and advanced movement strategies. The wheel drivetrain is used for the general forward and backward movement and is mechanically unilateral coupled to the shoulder drivetrain. In other words, if the shoulder is actuated, the kinematic coupling leads to a movement of the wheel as well, but not vice versa.

Wheel drivetrain—The wheel drivetrain, depicted as a sectional view in Figure 3, is actuated by a previously decribed motor unit, which is located in the center of the shoulder joint. The output motion of the motor unit is redirected in a bevel gear perpendicular with a ratio of 1:1 to an internal shaft inside the leg. The driving bevel gear is made of titanium 3.7164 and the driven bevel gear is made of 1.4548 stainless steel in condition H1150 for a dissimilar material approach. To provide enough structural integrity and, at the same time, a minimal thermal linkage between shoulder and Phobos surface, the internal running shaft and the structural outer pipe is made of titanium 3.7164. The material choice provides a compromise of stability, low thermal conductivity and weight. In result, the distance between shoulder and wheel axis amounts to 275 mm, which leads to an increased thermal expansion magnitude within the bearing arrangement of the internal shaft. Therefore this bearing arrangement is chosen to be most compliant to thermal stresses in a fixed-floating bearing arrangement. Located at the floating bearing, the pinion gear made of 1.4548 stainless steel in condition H1150, is attached to the internal shaft and drives the crown gear of the wheel output shaft. The crown gear is made of TECASINT 2391 and the stage has a ratio of 1:4.45. The pinion may move axial on the gear meshing of the crown gear, thus do not hindering its functionality and is most tolerant to thermal expansion. The wheel output shaft is mounted on a soft-preloaded bearing arrangement
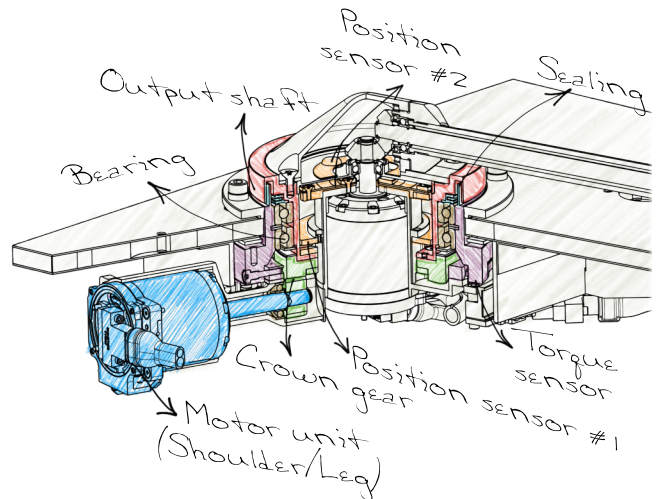

Figure 4: Shoulder drivetrain of Locomotion Subsystem

of angular contact ball bearings. Subsequent, a springed PTFE lip seal is used to protect the drivetrain from dust and contamination. To encounter also ESD related issues caused by static charge of Phobos surface, the sealing is made of an electrically conductive PTFE compound. In this way, no additional mechanisms, like slip rings, are necessary. Furthermore, surface damages on the raceways and balls of the bearings related to electrical discharge are avoided through isolating properties of the balls. Overall, the ratio of the drivetrain is 1:2227 and provides a uniform, extreme low traveling velocity and at the same time maintaining an adequate motor rotational speed [1]. The wheel shape is an optimized topology [8] to face different driving strategies and a broad range of Phobos surface scenarios, as far as yet known. Beside the optimized topology it provides a teethed interface for coupling it to the wheel drivetrain and interfaces at the grousers for the pillars of the hold down and release mechanism of the LSS, as later described.
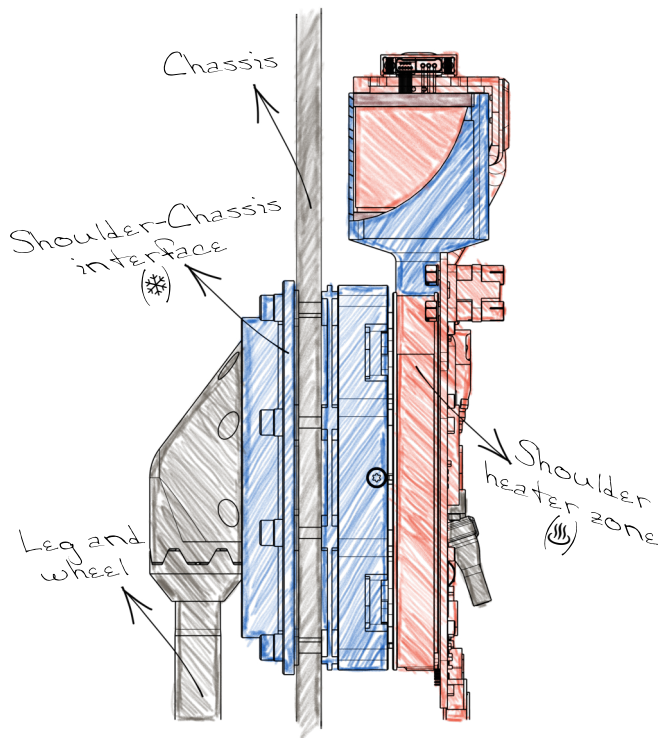
Figure 5: Thermal zones of the MMX Locomotion Shoulder

preloaded bearing arrangements to be most compliant to thermal gradients or the definition of different thermal zones inside the subsystem. The LSS can be divided into different thermal zones (see Figure 5), which are designed to reduce the heat leakage between the mechatronic components inside the rover and the external environment. The leg, wheel and the external parts of the shoulder-chassis interface module are directly exposed to the environmental conditions in space and on Phobos. As prior described, selected parts of the leg are made of titanium 3.7164. Although this is primarily due to mechanical reasons, the thermal design benefits from the low thermal conductivity of the material, which decreases the thermal conductance between the shoulder and the Phobos ground. In order to reduce the radiative heat transfer to the environment, it has been decided to use a surface coating. Surtec650 is selected for this purpose for all aluminium parts. It provides a suitable low IR emissivity and in addition also fulfills an additional role for the EMC grounding concept.

The shoulder can be divided into two main zones, as depicted in Figure 5: the shoulder-chassis interface and the heater zone, where the temperature-sensitive mechatronic components are located. The shoulder-chassis interface is thermally optimized by spacer bolts as well as isolation rings made from TECASINT 2011. Titanium screws are used to mount the locomotion shoulder to the chassis plate. In addition, the surface contact between the shoulder and chassis is also reduced through cutouts in the interface area. For the heater zone also insulating bodies are used to thermally decouple the mechatronic components from the rest of the shoulder as much as possible, while meeting the structural requirements for the mechanical assembly. The heater zone consists of

Shoulder drivetrain—The shoulder drivetrain, depicted as a sectional view in Figure 4, is systematically the same as the wheel drivetrain providing the same overall ratio, but requires no bevel gear stage. It is actuated by a motor unit, described in Section 2, which is located eccentric to the shoulder axis. A pinion gear, attached to the output shaft of the motor, driving the crown gear stage. The crown gear stage is identical to the one in the wheel drivetrain and is mounted on the shoulder output shaft, which is supported by a soft-preloaded bearing arrangement of angular contact ball bearings. Subsequent, a two stage sealing concept is realized: in the first stage a labyrinth sealing approach is used to cover coarse regolith, the second stage is a springed PTFE (electrically conductive) lip seal to protect the drivetrain from remaining fine dust particles.

Sensors

The shoulder unit is equipped with a strain-gauge based torque sensor to measure the loads acting around the shoulder axis in a range of ± 2 Nm and a FR4 based potentiometer as a position sensor for the alignment tasks, such as sun pointing. A second redundant polyimide foil based position sensor is implemented as well, but was decommissioned, due to signal instabilities at low temperatures. The sensors are described more detailed in the previous publications [1] and [2].

Thermal hardware

The mechanical design of the LSS was significantly influenced by the thermal requirements of the different harsh environments during the mission phases. In addition to the temperature limitations e.g. of the mechatronic components, adhesives and lubricants, other aspects such as thermal induced mechanical stress, or changes for ball bearing preloads had to be taken into consideration. To cope with these challenges, different measures are implemented, such as soft-

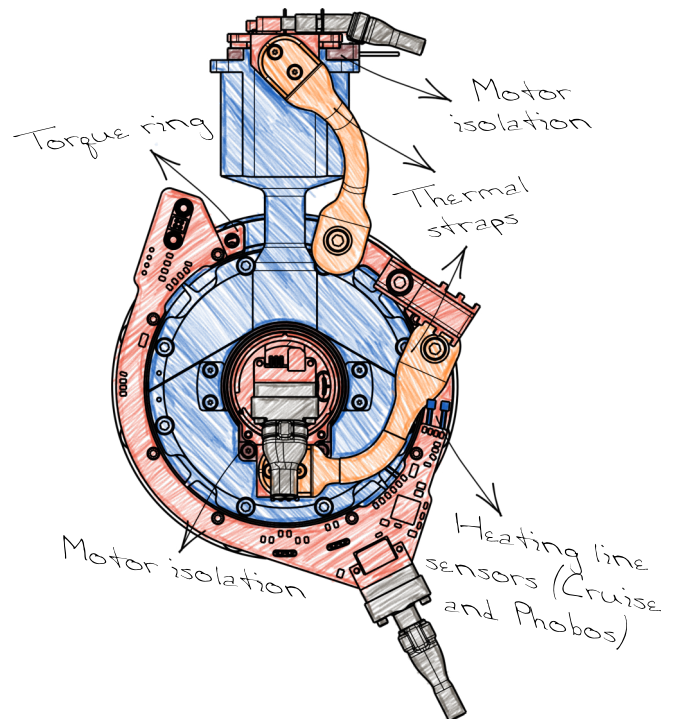**Figure 6**: Heater zone inside the MMX Rover

three double-layer heat foils. Each layer pair is used for the cruise heating line on the JAXA MMX spacecraft and the heating line on the MMX Rover. One is attached to the shoulder motor, one to wheel motor and one near the torque sensor board on the torque ring. In addition, the heat foils are covered with a reflective PET foil to reduce the radiative
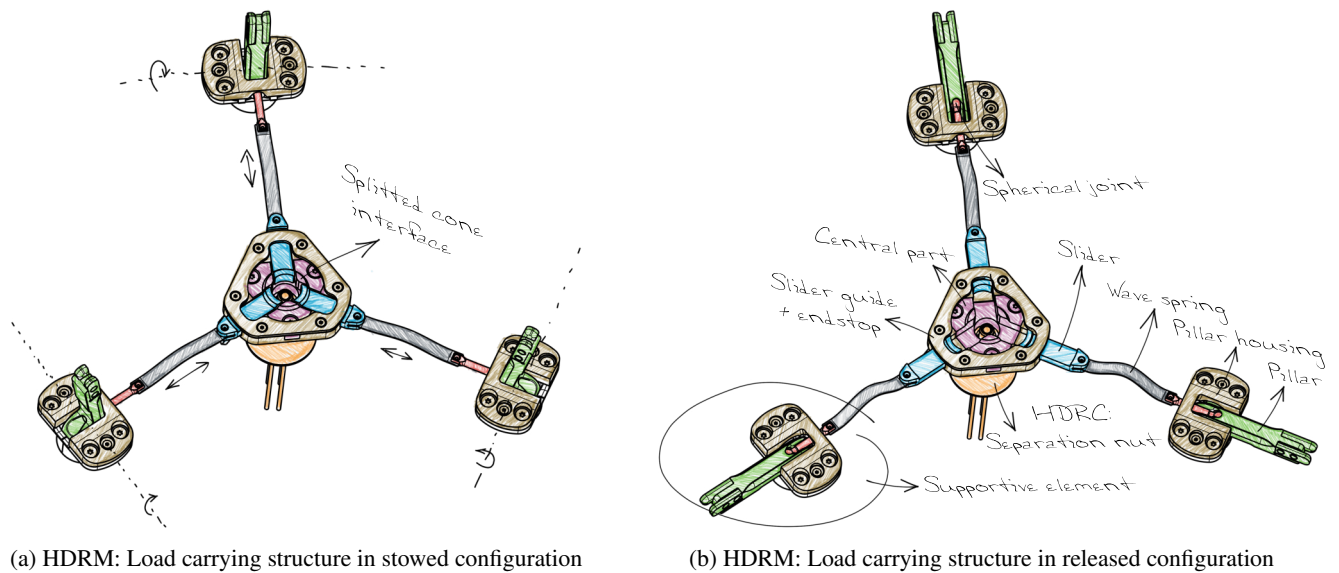
4

(a) HDRM: Load carrying structure in stowed configuration

(b) HDRM: Load carrying structure in released configuration

Figure 7: HDRM as mounted on the chassis side panel of the rover in released and stowed configuration

(a) HDRM: Cut view in stowed configuration

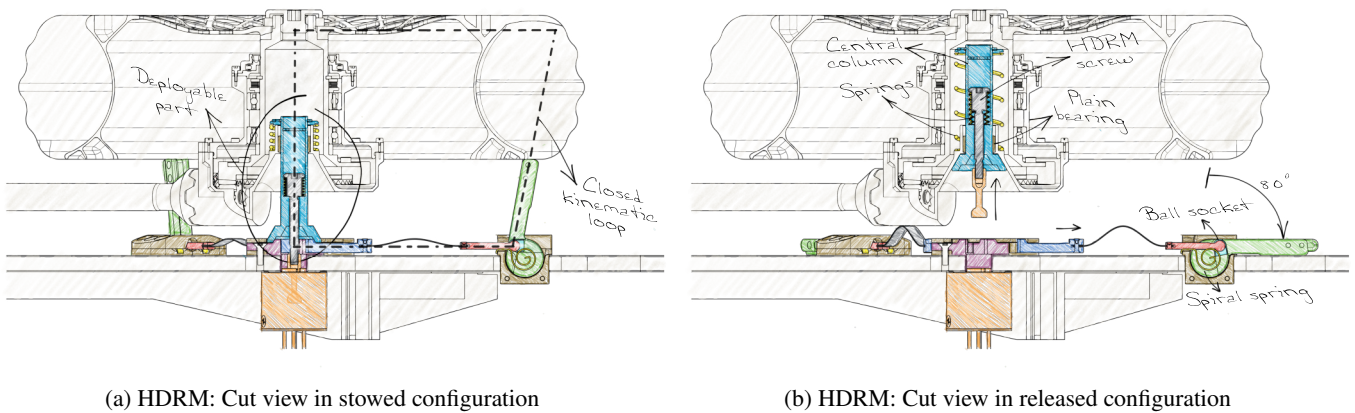(b) HDRM: Cut view in released configuration

Figure 8: HDRM as mounted on the chassis side panel of the rover in stowed and released configuration

heat exchange with the environment. A cylindrical part, the torque ring (see Figure 6), is specially designed to provide a suitable surface for mounting the heat foils, but also to increase the thermal capacity of the circuit board, resulting in a lower temperature rate change during heating cycles. Thermal straps are used to achieve a homogeneous thermal behavior between the heat foil areas. Each motor is connected to the torque ring.

Hold Down and Release Mechanism

The hold down and release mechanism (HDRM) of each locomotion unit comprises a load carrying structure (see Figure 7) and a deployable part (see Figure 8). The load carrying structure has a central static part with a splitted cone interface and a standard fuse-wired separation nut with a maximum preload of 1.3 kN, attached to side panel inside the rover. In addition three structural supportive mechanisms are evenly placed around the circumference of the central part. Each of the supportive mechanisms are composed of a slider guided in the static central part, a wave spring, a spherical joint and a structural supportive element, so-called pillar. The pillar has a spherical joint interface and is guided in an housing and actuated by two parallel spiral springs with

a total retraction torque of 0.25 Nm. The deployable part, shown in Figure 8, is located inside the wheel hub of the leg and is a spring-loaded shaft (retraction force of 53.5N) with a cup interface on its lower part. The shaft is guided in a cylindrical sleeve bearing for axial movement at release, thus providing the leg to maintain a fixed distance to the chassis side panel in stowed and released configuration. The shaft has a bore, in which a #6-32 UNJC-3A screw is placed to engage the deployable part to the load carrying structure at the splitted cone interface.

Furthermore, the sectional view of Figure 8 provides the HDRM in stowed and released configuration to explain the different states of the mechanism. At launch, flight and touchdown on Phobos, the locomotion subsystem is in stowed configuration (see Figure 8a). At this state, the leg and wheel is constrained in its motion by the splitted cone interface and the pillars to prevent over stress of the structural integrity and the drivetrains. The splitted cone interface is preloaded when the screw is tightened to the separation nut of the HDRC and besides holding the pillars through a form closure of the slider. The elastic element, the wave spring, is deflected and pulls the pillar through the spherical joint to his preloaded upright state as depicted in Figure 7a or Figure 8a. A spherical joint is chosen to obtain a most tolerant system

5

to the non-linear motions of the mechanism and machining tolerances of the chassis side plate. The ball joint and the pillar are made of titanium and are separated by an injection molded PVDF cup to provide lower friction. Additionally the effective distance between the force vector at the spherical joint and the pillar rotation axis is minimized to provide lower parasitic torques and thus increase the retraction torque of the pillars at release. Overall, this results in a hyperstatic state and is compensated by the elastic spokes of the wheel, leading to a closed kinematic loop through the wheel rim, the wheel spokes, the wheel hub, the deployable part and the load carrying structure. As a result, an increase of the overall stiffness of the system and an improvement against vibration and impact loads as required for this particular application is achieved.

After touchdown on Phobos the HDRM is released, as depicted in Figure 7b and Figure 8b, by burning the fuse-wire of the separation nut, leading to a retraction of the deployable part. Subsequently, the form closure at the cone interface of the slider is opened, resulting in the retraction of the three pillars at the rim of the wheel. The leg and wheel of the LSS is released and the operational task can be started.

3. TESTING

Before the actual operational tasks of the MMX rover on phobos begins, the LSS is subject to several loads of vibrational, thermal and ballistic nature. Within a period of two and a half years, extensive simulation and testing is performed to iterate the LSS subsequently and make it ready for the mission. A timeline shown in Figure 18 gives an idea of the testing done. In [1] and [2] the most important tests are highlighted, which led to major or minor design decisions of the system. Furthermore [3] is introducing the qualification and acceptance campaign of the QM/FM hardware. The following gives a more detailed description of the hardware setup and the most relevant tests regarding their load type, as well as the findings of each.

Hardware setup

For the qualification and acceptance campaign of the LSS one common hardware setup was designed to match the interfaces at the different test facilities. Except for the operational loads, all other loads were qualified and accepted with this setup to provide most representative conditions on subsystem level and a better mobility for the transport without the need of changing the configuration. The setup, depicted in Figure 9, consists of a frame for the interface of the facility, a chassis side panel and two locomotion units. The setups might differ due to planned utilization as described in Table 1 and therefore can be defined into three configurations.

The first configuration *QM1* is the most representative hardware setup on subsystem level. In contrast to the other configurations, a full chassis side panel, as it is used in the
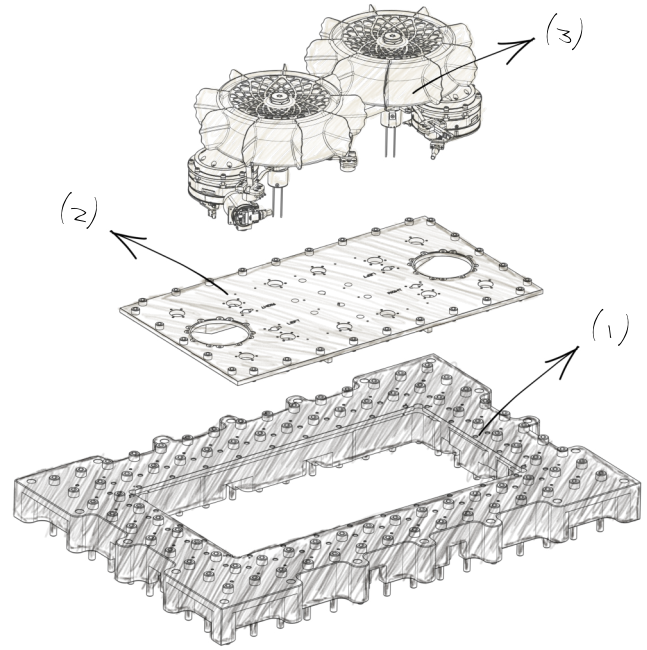

Figure 9: Hardware setup - interface frame (1), chassis side panel (2) and locomotion units (3)

rover, is utilized. The composite panel, made of aluminium honeycombs and carbon fibre top layers is clamped into the frame and the locomotion units are assembled to the side panel. This configuration was used to qualify the LSS for vibration and shock, but especially for the thermal requirements as it provides the most possible thermal environment at subsystem level.

The second configuration, which applies from *QM2* to *FS1*, is similar to latter configuration, but was utilized with a solid replacement panel made from aluminium 7075 and screwed to the frame, due to the lack of real chassis side panels at time. The hardware setup *QM2* was used to qualify the LSS for vibration, shock and thermal loads in the same configuration as the flight hardware. In this way the results of the acceptance of *FM1, FM2* and *FS1* could be compared. Additionally the hardware setup *QM2* was conducted in a delta qualification test for vibration loads and against impact loads.

The third configuration *QM3* was used to determine the required shock profile for the tests of *QM1* and *QM2*. It is similar to the second configuration, but the shoulders of the locomotion units were mass dummies.

Setup	Interface frame	Side panel	Hardware	Test				
				Vibr.	ΔVibr.	Shock	Thermal	Impact
Config. 1	for composite panel	Representative	QM1	●	○	●	●	○
Config. 2	for aluminium panel	Replacement	QM2	●	●	●	●	●
	for aluminium panel	Replacement	FM1	●	○	○	●	○
	for aluminium panel	Replacement	FM2	●	○	○	●	○
	for aluminium panel	Replacement	FS1	●	○	○	●	○
Config. 3	for aluminium panel	Replacement	QM3	○	○	●	○	○

Table 1: Hardware setups for qualification and acceptance campaign
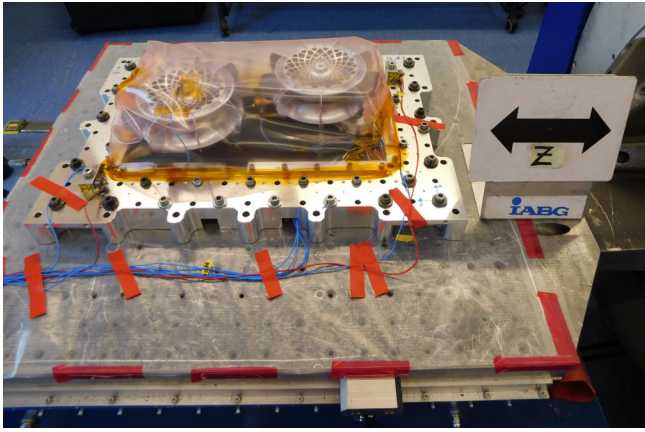
Figure 10: Hardware setup on interface plate of shaker facility

Figure 11: Discrepancy at resonance frequency of 270 Hz in y-axis between qualification and flight model

Vibration and shock load

At launch the LSS will face vibration and shock loads, thus the objective is to protect the sensitive parts of the subsystem from damage and the drivetrains from degradation. The loads were obtained by the expected launcher profile, the structural couplings in the rover and the contributions of other subsystems. A previous and initial test was performed on the engineering model of the LSS to obtain the general system behavior and to investigate the overall need of the pillar design as a structural supportive element. Based on the findings, several design decisions were made, which were described in [2]. Subsequently, three follow up tests were conducted as part of the qualification and acceptance campaign. The first test covered the vibration and shock at qualification level, the second test the vibration at acceptance level and the third test was a delta qualification test.

As stated, the first test covered the vibration and shock at qualification level and was conducted with the two setups *QM1* and *QM2*, as described in Table 1. Both hardware setups were prepared by a visual check and the application of acceleration sensors for the shaker and shock facility. The position of the sensors were obtained beforehand by a detailed modal analysis of the LSS, where the parts which contributes with more than 10 % of the effective mass at found resonance frequencies. After the application, the setups were screwed to the interface plate of the facility as shown in Figure 10 and were charged with sine and random loads for each axis. An overview of the applied loads are given in [3]. Before and after applied load, the resonance profile of the setup was checked to detect any possible degradation of the device under test. At the end of the vibration tests, the setups were mounted to the interface of the shock facility and charged with a shock load three times in each axis. In conclusion, the shock criteria were fulfilled, the vibration criteria of a frequency shift of less than 5 % and amplitude shift of less than 20 % could not be hold in each axis due to the properties of the HDRM. However, the integrity of the LSS was shown through successful HDRM releases and functionality test right before the following thermal tests.

The second test, the acceptance of the flight model, was conducted in the same way as the qualification, but with lower loads and durations. Also no shock load was applied on the flight model hardware of the setups *FM1*, *FM2* and *FS1*. During the vibration tests on the y-axis, a non-conformance between the qualification model and the flight model resonance at 270 Hz was investigated as shown in Figure 11. Whereas the flight model showed a distinctive frequency at
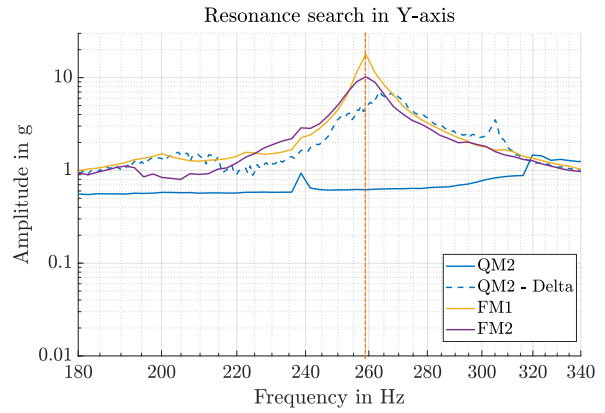
270 Hz, the qualification model shows a negligible amplitude, although the frequency should be existing from the modal analysis. As two possible states exists, with and without the designated frequency, a third test (delta qualification test) with the hardware setup *QM2* was performed, as it is identical to the flight model. A full vibration qualification was conducted on the setup and it was possible to reproduce the 270 Hz on this model. The issue was found in the assembly procedure, when the HDRM is engaged and was resolved through an updated procedure for aligning the central column of the deployable part to the load carrying part of the HDRM. After the test a defect in both torque sensors was observed. During inspection no structural damage was found, but a microscopic analysis revealed an internal damage in the applied strain gauges of the torque sensor. The other qualification and acceptance models integrity was shown through multiple subsequent functional tests and visual inspections between each test during the campaign. An additional functional test confirmed further the healthy state of the torque sensor in the flight model. The qualification and flight model were therefore released for further operation. It is noted, that the torque sensors are only be used to detect a situation of a blocked LSS during operation and therefore only reduce the anomaly detection capabilities in case of failure.
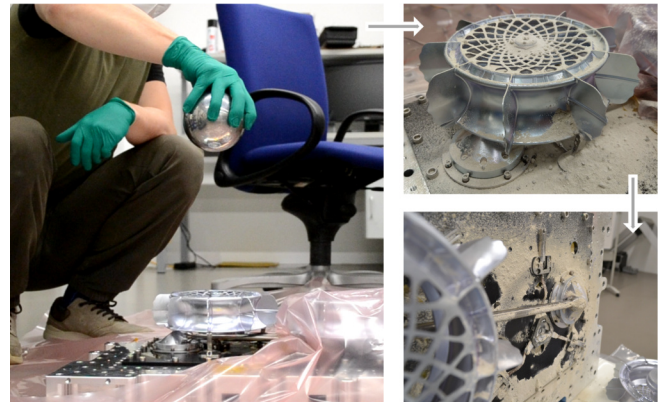

Figure 12: Cold impact and dust release test

Impact load

During the touchdown phase of the mission, the LSS has a high probability to be the initial point of contact as an exposed
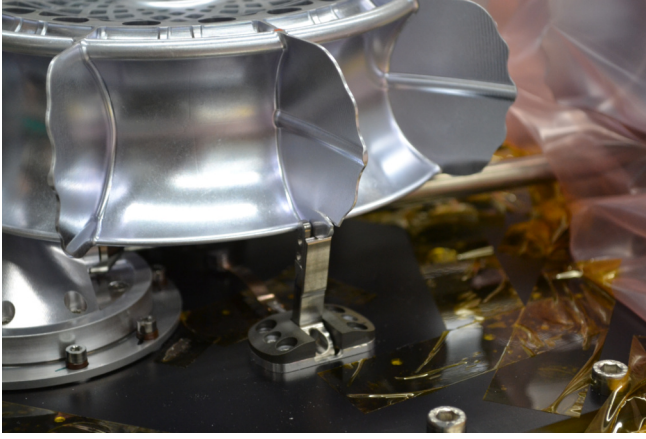
Figure 13: Damage on wheel grouser of locomotion unit tested at ambient

Table 2: TRP1 and TRP2 thermal environment for locomotion modules. The ()* indicates temperatures that are varied for the four QM modules.

	TRP1 [°C]		TRP2 [°C]	
	min	max	min	max
non OP	−125	+85	−80*	+85
OP Phobos	−100*	+70	−35	+80
OP Cruise	−125	+70	−35	+70
HDRM release	−110	+70	−35	+70

part of the rover. When the spacecraft reaches Phobos, the rover is planned to be dropped about 50 m above the surface with a colliding velocity of around $0.9 \, \mathrm{ms^{-1}}$. Therefore, the expected energy at impact sums up to approximately 10.1 J, which needs to be encountered by the mechanical structure of the LSS. As the kinematic energy may cause considerable damage without any precautions, two different approaches were investigated.

The first approach accounted for a landing platform as described in [1] to protect the whole rover including the LSS and deploys after ballistic landing. As described in the publication, the mass for such a system is not affordable and is therefore not realized.

The second approach consist of a local reinforcement of the LSS through the HDRM, as described prior, leading to a more complex, but lighter solution. Within the project, the ballistic landing scenario was tested in three dedicated tests, at which the chronological first two ones are shortly described by their setup and their findings in [2].

The third and last test was conducted on the locomotion units of the hardware setup *QM2* after the vibration, shock, release, thermal, performance and lifetime tests of the qualification campaign are finished. Hereinafter, the HDRM of the prestressed hardware was refurbished and the locomotion units were engaged again in stowed configuration for the impact test. At first, both locomotion units were charged with a falling weight of 4 kg from a height of 25 cm, with the addition that the first locomotion unit was charged at ambient and the second locomotion unit at −125 °C. Subsequent a visual inspection without touching the setup was performed. After inspection, the units were contaminated with dust of different grain size and released afterwards as shown in the sequence Figure 12 to provide a more realistic scenario. Finally a full functional test and inspection, including dismounting, was applied to check the complete hardware on potential damages. The inspection revealed a tear in the grouser of the wheel directly below the collision point as shown in Figure 13, caused by the impact, but do not hinder the functionality of the drive or the HDRM as later proofed. The detailed inspection and dismounting of the hardware moreover did not show any damages on the locomotion units, which originates from the impact test.

Thermal load

The thermal condition of the LSS varies depending on the mission phases and the operational conditions. In order to verify the functionality under the different thermal conditions, multiple thermal test campaigns have been executed. For example, during the engineering phase, the release functions of the HDRM prototype was tested in the thermal vacuum chamber (TVAC) at low temperatures around −140 °C. Within the test, it was found that the pillars of the HDRM could block the release due to thermal expansion of the structural parts. Based on these results, the mechanical design was optimized to the given conditions for the QM.

One more of the essential thermal verifications is the thermal cycling test of the QM Locomotion modules. The temperature ranges for this test were specified considering the different mission phases and operational conditions as summarized in Table 2. Since the LSS are mounted on the rover chassis, which is exposed to the surrounding environment, the temperatures of the mechanical interface and the external part of the LSS vary significantly during the cruise phase. For surviving the cold environment, the dedicated cruise heater line from the MMX spacecraft supports the temperature maintenance. In order to be consistent with the limited heating power, only the temperature critical components, such as motors and the PCB, are temperature controlled by the cruise heater. The other mechanical components, including HDRM, are subject to the harsh thermal environment. Corresponding to this design concept, two different temperature ranges were specified as shown in Table 2, where TRP2 represents the motor and PCB temperatures and TRP1 represents the shoulder-chassis interface temperature of the LSS (see Figure 5). For the landing operation, the rover is planned to be pre-heated before the separation and the HDRM will be activated shortly after the landing. However, it is not realistic to precisely predict the HDRM temperature at the activation, because it depends on the detailed operational timeline and the actual Phobos environment. Therefore, on the subsystem level qualification, the HDRM release was tested for both high and low temperature conditions as shown in Table 2. On Phobos, the LSS temperatures are maintained by the heaters to endure the cold Phobos environment, especially during the night period. Because of the stringent power budget of the rover system, it may be necessary to lower the survival temperature compared to that of cruise phase. The TRP2 non-op minimum temperature of −80 °C in Table 2 represents the possible survival temperature on Phobos with the qualification margin. The heaters are also planned to be used to preheat the LSS to reach the operational level for the motor operation. Eventually, through the QM thermal cycling campaign, the LSS was verified for the wide temperature range, which corresponds to the thermal conditions of the cruise, Phobos and HDRM release operations. At this time simulations and test are still ongoing, such that further details to the thermal test campaign are planned to be released in a dedicated future work.

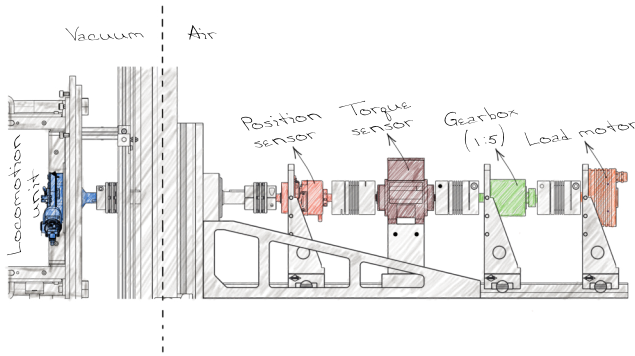| Cycle Nr.	TRP1* [°C]	TRP2 [°C]
1	ambient	ambient
2	+65	80
3	TVAC min	-35
4	TVAC min	-30
5	TVAC min	-20
6	TVAC min	-10
7	TVAC min	-0

Table 3: Cycles during test

Figure 14: Sensor setup on the rotary feed through

Operational load

After landing, the rover will have to upright itself and point its solar panels towards the sun. The LSS has to be able to lift and flip the rover to its upright orientation even when the wheels are buried in sand or the movement is restricted by lager rocks. To ensure the performance of the LSS, a load test under operational conditions was conducted in a thermal vacuum chamber (TVAC). Due to the long duration of the test only one module of *QM1* was tested.

To avoid a complex setup and because the used thermal chamber has only one rotary feed through, the test of the shoulder and wheel actuator was conducted separately. Therefore the *QM1* module had to be reconfigured for each test. For the wheel actuator test, the shoulder was mounted on the thermal regulator plate with a can-like adapter and the wheel hub was fixed in alignment to the rotary feed through. Instead of the wheel an adapter was used to connect the drivetrain to the feed through. For the shoulder actuator the whole leg was dismounted and again an adapter was used to transfer the rotational motion to the feed through.

	Req. Torque [Nm]	Margin	Friction torque [Nm]	Margin	Total [Nm]	Load cases [Nm]
Wheel	0.5	3	0.33	3	2.5	0, 1.25, 2.5
Shoulder	1.5	1.73	0.8	3	5	0, 2.5, 5

Table 4: Components of applied load torques

	Rotor RPM	Link RPM	Wheel velocity [mm/s]
Slow	14.82	0.0066	0.0705
Middle	240.65	0.1082	1.144
Fast	2199.88	0.9887	10.457

Table 5: Different speeds tested

During this test the LSS was monitored in regard to power consumption, thermal behavior, output velocity and torque. For the external sensors a Heidenhain ERN480 position and Torquemaster TM306 torque sensor were chosen. They were mounted on an rail system aligned with the rotary feed through, see Figure 14. In addition a motor with a 1:5 gearbox was added to apply the expected loads. The electrical parameters were measured with a Keithley DAQ6510 multimeter and by reading out the power supply values. The thermal behavior was monitored with several sensors applied to the TRPs, but also to other points of interest. The external sensors were connected via Ethernet or USB bus. The test sequences were all automated and controlled by a PC running a python script. It included a no-load motion before and after each thermal cycle, a no load speed accuracy test, constant torque cases seen in Table 4 with different speeds listed in Table 5, ramping torques with and against the driving direction and a maximum load torque movement over a rotation of 400deg.

Thermal simulation showed that the TRP1 would reach −95 °C at beginning of operations. The used TVAC however was only capable to cool down to −70 °C. This limitation was overcome by directly connecting the shoulder to the thermal regulator plate without any thermal isolation parts. To validate if the internal temperatures of motors and the electronics are met, a TRP1* was defined that is located on the inner side of the isolation ring opposing TRP1. FEM simulation indicated that TRP1* reaches −80 °C to −69 °C at the beginning of operation. It however raised from −71 °C to −61 °C after 10 min, so the test represented a slightly delayed operation startup. So the internal temperatures were representative for the operation conditions, but the leg and wheel were tested under warmer temperatures. The biggest impact of the deviation was the smaller sealing friction in the wheel hub and the shoulder. This was compensated by extrapolating previously recorded sealing friction data to the expected temperatures and adding the resulting torque to the test load, see Table 4. During the test the heaters were actively
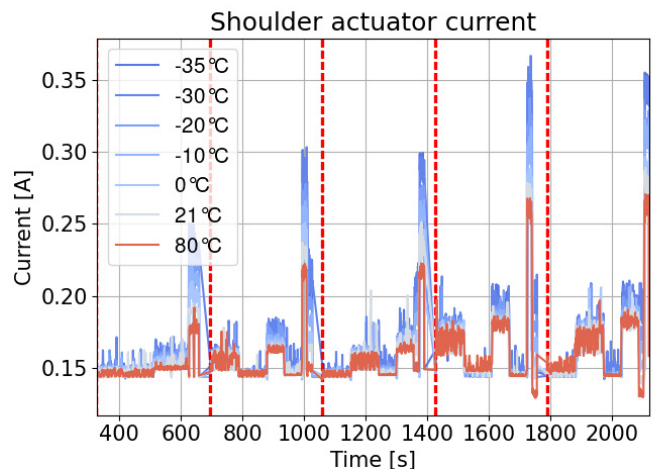
Figure 15: Shoulder actuator currents for the different TRP2 temperature cases. Left to right: 0 Nm, 2.5 Nm, −2.5 Nm, 5 Nm, −5 Nm, each case with the three speeds

controlled to keep especially TRP2 in the specified range. The defined temperatures cases could be seen in Table 3. The different TRP2 temperatures were chosen to monitor the friction of the motor in warmer temperatures. It also increased the thermal gradient in the shoulder, which stress tests the internal parts.

Figure 15 shows the change in the current draw at different

TRP2 temperatures during the constant torque cycles. It is clearly visible that at colder temperatures more power is consumed. This was expected since viscosity of the lubrication in the HD gearing increases. With the wheel setup higher startup currents at high load and speed were detected. However the current limit of 1 A was never reached.
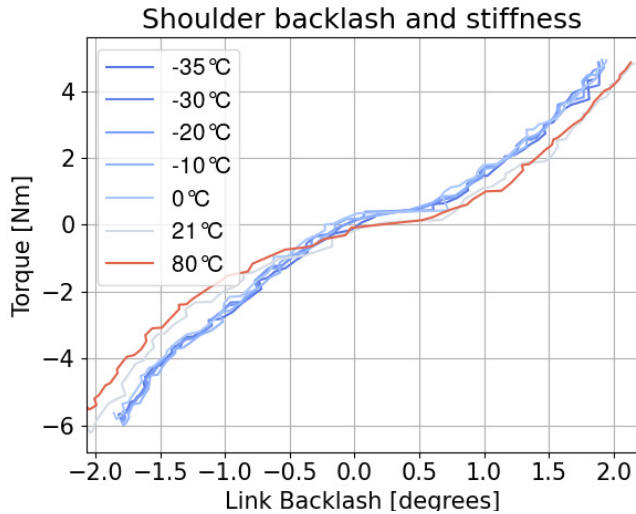
Figure 16: Movement on the external position sensor in relation to the applied load, while motor is stationary
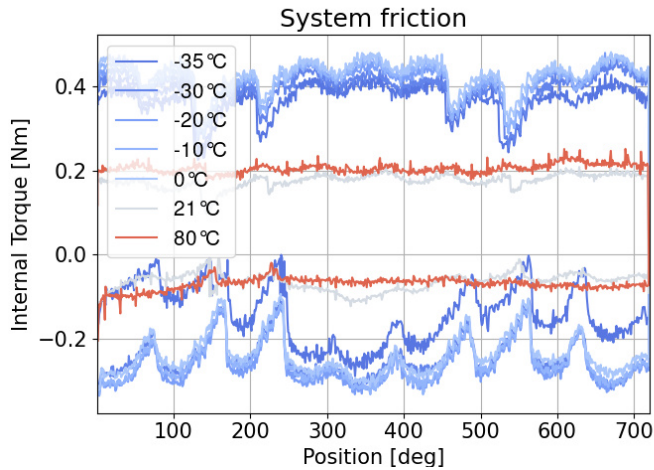
Figure 17: Comparison of the measured internal and reference torque

The stiffness and backlash of the shoulder can be evaluated with the load transition from negative to positive torque during high load full rotation test. At this point the motor is not moving, so the calculated angle difference on the link side includes the backlash of all three gear stages, as well as the compliance of all parts in the drive train. Figure 16 shows the relation of deflection on the external position sensor and the applied load. It is clearly visible that there is a plateau at zero torque and deflection. This is the main backlash in the first gear stage. With increasing torque the deflection gets more linear, suggesting a elastic deformation of the drive train components.

The friction of the bearing and sealing in the shoulder was also determined, see Figure 17. The plotted data was recorded during the no load cycle and shows the expected friction at ambient and during the hot case. At colder temperatures however big ripples in the measurement were noticeable. It was most likely caused by an expansion of the inner part of the shoulders bearing assembly, due to a bad thermal connection to the thermal regulator plate. This led to a force on the crown gear of the motor and therefore an axial load on the inner ring of the torque sensor, which furthermore deformed the strain gauges of the torque sensor in a non intended way and interferes the measurement.

In conclusion the LSS performed as expected with no signs of degradation. The test equipment also performed as expected, however the gearbox on the load motor increased the torque fluctuation and the no real-time communication led to some noise in the measurements. Since the LSS is driven with very low speeds this had a minor impact on the measurement quality.

4. CONCLUSION

The mechanics of the Locomotion Subsystem is aimed to cope with several loads in a harsh environment during the MMX mission. Not only it has to be resilient to vibration, thermal and operational loads, but also impact loads have to be considered in a milli-g environment. Naturally, a low gravity environment seems to be a relaxation in the requirements on the rovers structural integrity, but concludes in a complex compromise of the system stiffness targeting vibrational and ballistical loads, if no landing platform is utilized. Taking this in consideration, the mechanical structure of the LSS and its sub-components are described and specific design decisions are explained. Beside the drivetrains, a novel hold down and release mechanism is presented to protect the drivetrains of the LSS and cope at the same time with different kind of loads. Finally, the resilience of the subsystem has been verified in several tests according to the requirements of the mission. However, there are still subjects for further improvements with respect to future missions: like an improved motor unit towards cryogenic motor operation by providing a full dry-run capability of the gearing.

Currently, the flight model of the LSS is integrated successfully in the rover flight chassis. The next step is the acceptance of the complete rover hardware, including the LSS, to be tested on system level, before finally released to Phobos.

REFERENCES

[1] H.-J. Sedlmayr, S. Barthelmes, R. Bayer, W. Bertleff, M. Bihler, F. Buse, M. Chalon, D. Franke, F. Ginner, V. Langofer, R. Lichtenheldt, T. Obermeier, A. Pignède, J. Reill, and J. Skibbe, "MMX – Development of a Rover Locomotion System for Phobos," in *Proceedings of the IEEE Aerospace Conference*, 2020.

[2] S. Barthelmes, T. Bahls, R. Bayer, W. Bertleff, M. Bihler, F. Buse, M. Chalon, F. Hacker, R. Holderried, V. Langofer, R. Lichtenheldt, S. Moser, K. Sasaki, H.-J. Sedlmayr, J. Skibbe, L. Stubbig, and B. Vodermayer, "MMX Rover Locomotion System - Development and Testing towards the Flight Model," in *Proceedings of the IEEE Aerospace Conference*, 2022.

[3] S. Barthelmes, R. Bayer, W. Bertleff, M. Bihler, F. Buse, M. Chalon, F. Hacker, G. Geyer, C. Hofmann, R. Holderried, A. Kolb, E. Krämer, V. Langofer, R. Lichtenheldt, S. Moser, K. Sasaki, H.-J. Sedlmayr, J. Skibbe, L. Stubbig, and B. Vodermayer, "Qualification of the MMX Rover Locomotion Subsystem for the Martian Moon Phobos," in *Proceedings of the IEEE Aerospace Conference*, 2023.

[4] M. Chalon, M. Maier, W. Bertleff, A. Beyer, R. Bayer, W. Friedl, P. Neugebauer, T. Obermeier, H.-J. Sedlmayr, N. Seitz, and A. Stemmer, "Spacehand: a multi-fingered robotic hand for space," in *Proceedings of the ASTRA Conference*, 2015.

[5] J. Reill, H.-J. Sedlmayr, S. Kuß, P. Neugebauer, M. Maier, A. Gibbesch, B. Schäfer, and A. Albu-Schäffer, "Development of a mobility drive unit for low gravity planetary body exploration," in *Proceedings of the ASTRA Conference*, 2013.

[6] J. Reill, H.-J. Sedlmayr, P. Neugebauer, M. Maier, E. Krämer, and R. Lichtenheldt, "MASCOT - Asteroid lander with innovative mobility mechanism," in *Proceedings of the ASTRA Conference*, 2015.

[7] M. Iskandar and S. Wolf, "Dynamic friction model with thermal and load dependency: modeling, compensation, and external force estimation," in *2019 International Conference on Robotics and Automation (ICRA)*. IEEE, 2019, pp. 7367–7373.

[8] L. Stubbig and R. Lichtenheldt, "Optimizing the shape of planetary rover wheels using the discrete element method and bayesian optimization," in *VII International Conference on Particle-based Methods – Particles*, 2021.

BIOGRAPHY

Viktor Langofer received the degrees of B.Sc. and M.Sc. from Technische Universität Kaiserslautern. Since 2017, he has been Research Associate at German Aerospace Center (DLR), Institute of Robotics and Mechatronics. His main area of activities are research in compliant and tendondriven mechanisms in humanoid robotics, as well actuators design for space applications. He is responsible for the mechanical design of the locomotion subsystem of the MMX rover.

Ralph Bayer received his Master of Science (M.Sc) in Mechanical Engineering from the Regensburg University of Applied Sciences, Germany, in 2011 and joined the German Aerospace Center (DLR) in 2010. He was a member of the development team of the space qualified force feedback joystick used for the KONTUR-2 ISS-to-ground telemanipulation experiments in 2015-2016, as well as the METERON SUPVIS Justin ISS-to-ground telerobotic experiments in 2017–2018. He currently serves as the lead thermal engineer at DLR's Institute of Robotics and Mechatronics. Mr. Bayer plays a key role in the thermal design of the MMX locomotion system.

Alexander Kolb graduated as an Dipl.Ing. in mechatronics from the University of Innsbruck, Austria in 2019. Since then he has been working at the German Aerospace Center (DLR), Institute of Robotics and Mechatronics as an mechanical engineer. He did his first work in the field of medical robotics, transitioning to space domain in 2020. His research focus lies on the optimization of electromechanical actuators.

Kaname Sasaki received his Master degree in Aerospace Engineering from Tokyo University, Japan. Since 2013 he works at the department of Mechanics and Thermal Systems of the DLR Institute of Space Systems in Bremen, Germany. He contributed to the development and operation of the asteroid lander MASCOT and the DLR payload HP³ as part of the NASA/JPL Mission INSIGHT. Currently, he is involved in the thermal design and analysis of the Locomotion subsystem in the MMX rover project.

APPENDICES

A. MATERIALS

An overview of the chosen materials in correspond to the referenced figures.

Reference	Part	Material
Figure 2	Bearings (balls)	SI3N4
	Bearings (cage)	Vespel SP3
	Bearings (rings)	1.4108
	Harmonic drive	div.
	Heater	PI/Copper
	Planetary gear (planet)	TECASINT 2391
	Planetary gear (ring)	1.4548 H1150
	Planetary gear (sun)	1.4548 H1150
	Stator and rotor	div.
Figure 3	Bearings (balls)	SI3N4
	Bearings (cage)	Vespel SP3
	Bearings (rings)	1.4108
	Bevel gear (drive)	3.7164
	Bevel gear (driven)	1.4548 H1150
	Crown gear	TECASINT 2391
	Crown gear (pinion)	1.4548 H1150
	Feedthrough shaft	3.7164
	Sealing	Conductive PTFE
	Wheel	7150-T7751
Figure 4	Bearings (balls)	SI3N4
	Bearings (cage)	Vespel SP3
	Bearings (rings)	1.4108
	Crown gear	TECASINT 2391
	Crown gear (pinion)	1.4548 H1150
	Output shaft	7075
	Position sensor #1	FR4
	Position sensor #2	PI
	Sealing	Conductive PTFE
	Torque Sensor	7075
Figure 6	Torque ring	7075
	Motor isolation	TECASINT 2011
	Thermal straps	Copper
Figure 7	Central part	7075
	Slider endstop	TECASINT 2391
	Slider guide	TECASINT 2391
	Slider	7075
	Wave spring	1.4310
	Pillar housing (top)	TECASINT 2391
	Pillar housing (bottom)	7075
	Pillar	3.7164
	Spherical joint	3.7164
	Spherical joint (sleeve)	PVDF
Figure 8	Central column	3.7164
	HDRM screw	1.4548 H1150
	Springs	1.4310
	Plain bearing	DP4
	Spiral spring	1.4310

Table 6: Materials

B. TESTING TIMELINE

Thermal test of motor unit
Identify power consumption in temperature range from -60 to +60°C

2019
2020

Impact test of first HDRM prototype
Proof of concept for touchdown scenario on phobos

Thermal vaccum test of motor unit
Characterisation of motor unit under full environmental conditions

Thermal vaccuum test of locomotion
Characterisation of locomotion unit under full environmental conditions

Operational terrain test
Rover dummy with full equipped locomotion subsystem driving on different soil conditions

Full rover droptest
Simulation of touchdown on phobos as proof of concept and identifcation of forces

2021

HDRM functional test
HDRM release at expected cold and vacuum environment

Wheel traction test
Verification of wheel concept

Shaker test
Vibration test of locomotion subsystem with and without HDRM pillars

Deep temperature test
Out of specs storage temperature of motor units below -150°C

Impact test of iterated HDRM
Identification of last structural weaknesses

Sealing friction test
Characterisation of the torque behaviour of the sealings at different speeds and temperatures

Thermal functional test
Characterisation of the drivetrains at different loads, speeds and temperatures

Thermal balance test
Correlation of thermal model with physical setup

Dust break-in test
Verification of sealing concept

Structural Model test
Full rover test campaign under certain mission loads and environments

HDRM release lab test
Testing final HDRM design

2022

Vibration/Shock qualification test
Qualification of locomotion subsystem to vibration and shock loads

Thermal qualification test
Qualification of locomotion subsystem to thermal loads

Performance and life qualification test
Qualification of locomotion subsystem to expected loads and speeds at different temperatures and mission parameters

Vibration acceptance test
Acceptance of locomotion subsystem flight model to vibration loads

Cold impact and HDRM release test
Most realistic simulation of touchdown on phobos including impact, contamination with dust and release at -130°C

Thermal acceptance test
Acceptance of locomotion subsystem flight model to thermal loads

Figure 18: Timeline of relevant tests